Effects of dark energy on dynamic phase transition of charged AdS black holes

Shan-Quan Lan, Jie-Xiong Mo,* Gu-Qiang Li, and Xiao-Bao Xu
Institute of Theoretical Physics, Lingnan Normal University, Zhanjiang, 524048 Guangdong, China

(Received 23 April 2021; accepted 19 October 2021; published 12 November 2021)

In a search for the effects of quintessence dark energy on the kinetics of black hole phase transition, we investigate in detail the dynamic phase transition of charged anti–de Sitter black holes surrounded by quintessence in this paper. We compare the case with dark energy and the case without dark energy. It is shown that the initial black hole state evolves more quickly in the case with dark energy than in the case without dark energy, no matter what the initial black hole state is. The result concerning the first passage process further supports this finding. The transition from the large (small) black hole state to the small (large) black hole state happens quickly. Last but not least, we calculate the mean first passage time for various choices of parameter ω_q. It is shown that the mean first passage time for the case with dark energy is much shorter than that of the case without dark energy, which can be understood by the result that the height of the barrier of Gibbs free energy for the case with dark energy is lower than that of the case without dark energy. Interestingly enough, the effect of dark energy is quite unique. For the range of ω_q, there exists a minimum mean first passage time. With the increasing of ω_q from -0.99 to -0.34, the mean first passage time decreases dramatically and then increases. Considering the mean first passage time is an observable of black hole dynamic phase transition, the unique results we obtain here may shed new light on constraining the parameters of the quintessence dark energy theory based on future observations.

DOI: 10.1103/PhysRevD.104.104032

I. INTRODUCTION

Thermodynamics, especially the phase transition of anti–de Sitter (AdS) black holes, has received increasing attention in the past decade. From the perspective of the extended phase space [1–3] including both the thermodynamic pressure and the volume as variables, Kubizňák and Mann investigated the P-V criticality of charged AdS black holes [4] and further enhanced the analogy between charged AdS black holes and liquid-gas system observed previously by Chamblin *et al.* [5,6]. Extensive intriguing phenomena of AdS black holes have been disclosed, such as reentrant phase transition [7], triple point phase transition [8,9], λ-line phase transition [10], and N-fold reentrant phase transition [11], which seems to suggest that AdS black holes share similarities with everyday thermodynamic systems. There are so many references in the literature that we are not able to list them all here; for reviews covering this research field, see Refs. [12,13].

Although a variety of results associated with the phase transition of AdS black holes have been reported, the underlying kinetics of black hole phase transition remained a mystery until Li and Wang *et al.* attempted to crack this tough problem recently [14,15]. Based on the free energy landscape, their works shed some light on both the dynamic process of the Hawing-Page phase transition [14] and the van der Waals-like phase transition [15]. For Schwarzschild AdS black holes, it was found that a black hole or AdS space has the chance to transition from one phase to another due to thermal fluctuations. By studying the Fokker-Planck equation, the probabilistic evolution was probed with the mean first passage time derived in [14]. Similarly, for Reissner-Nordström-AdS (RN-AdS) black holes, the large black hole phase and the small black hole phase can transition to each other due to thermal fluctuation. The first passage process was studied in detail [15].

These pioneering works were subsequently generalized to the case of four-dimensional Gauss-Bonnet AdS black holes [16] and five-dimensional neutral Gauss-Bonnet AdS black holes [17]. More interestingly, Wei *et al.* probed the dynamic process at a black hole triple point [18] and found that the initial large, intermediate, or small black holes can switch to other coexistent phases. Very recently, Li *et al.* investigated the turnover of the kinetics for the charged AdS black hole phase transition [19], providing a novel way to probe the black hole microstructure.

In the former work done by one of us [20], the P-V criticality of charged AdS black holes surrounded by quintessence was investigated in the extended phase space where the cosmological constant is viewed as a variable, and identified as thermodynamic pressure. It was shown

*Corresponding author.
mojiexiong@gmail.com

 © 2021 American Physical Society

that quintessence dark energy affects the critical physical quantities. Inspired by the works dealing with the kinetics of black hole phase transition mentioned above, it would certainly be interesting to probe the dynamic phase transition of charged AdS black holes surrounded by quintessence. First, we can gain a dynamical picture for the phase transition of charged AdS black holes surrounded by quintessence, from which the effects of dark energy on the black hole phase transition would be more clear. Second, this generalization will help check whether the treatment proposed in the pioneering works of black hole dynamic phase transition is universal or not. Last but not least, dark energy is also of enough interest in itself; dark energy serves as a theoretical candidate to explain why the Universe is expanding with acceleration. As one of the dark energy models, quintessence [21] may explain the late-time cosmic acceleration [22–25]. Both the black holes surrounded by quintessence and their thermodynamic properties have gained considerable interest [26–42].

The organization of this paper is as follows. A brief review of thermodynamics especially P-V criticality concerning the RN-AdS black hole surrounded by quintessence will be presented in Sec. II. Dynamic phase transition of the RN-AdS black hole surrounded by quintessence will be investigated in Sec. III, where we will focus on the Gibbs free energy landscape, probabilistic evolution, and the first passage process in three subsections, respectively. We will end this paper with conclusions in Sec. IV.

II. A BRIEF REVIEW ON P-V CRITICALITY OF THE RN-ADS BLACK HOLE SURROUNDED BY QUINTESSENCE

The metric of the RN-AdS black hole surrounded by quintessence reads [26]

$$ds^2 = f(r)dt^2 - f(r)^{-1}dr^2 - r^2(d\theta^2 + \sin^2\theta d\varphi^2), \tag{1}$$

where

$$f(r) = 1 - \frac{2M}{r} + \frac{Q^2}{r^2} - \frac{a}{r^{3\omega_q+1}} - \frac{\Lambda r^2}{3}. \tag{2}$$

The effect of quintessence dark energy is reflected in the fourth term of the above expression, where ω_q is the state parameter of quintessence dark energy satisfying the relation $-1 < \omega_q < -1/3$. a is the normalization factor which is related to the density of quintessence ρ_q via

$$\rho_q = -\frac{a}{2}\frac{3\omega_q}{r^{3(\omega_q+1)}}. \tag{3}$$

The mass of the black hole M, the Hawking temperature T, and the entropy S can be derived as

$$M = \frac{r_+}{2}\left(1 + \frac{Q^2}{r_+^2} - \frac{a}{r_+^{3\omega_q+1}} - \frac{\Lambda r_+^2}{3}\right), \tag{4}$$

$$T = \frac{f'(r_+)}{4\pi} = \frac{1}{4\pi}\left(\frac{1}{r_+} - \frac{Q^2}{r_+^3} + \frac{3a\omega_q}{r_+^{2+3\omega_q}} - r_+\Lambda\right), \tag{5}$$

$$S = \int_0^{r_+}\frac{1}{T}\left(\frac{\partial M}{\partial r_+}\right)dr_+ = \pi r_+^2. \tag{6}$$

Treating the cosmological constant as thermodynamic pressure allows us to work in the extended phase space with the thermodynamic pressure P and thermodynamic volume V as

$$P = -\frac{\Lambda}{8\pi}, \tag{7}$$

$$V = \left(\frac{\partial M}{\partial P}\right)_{S,Q} = \frac{4\pi r_+^3}{3}. \tag{8}$$

The Gibbs free energy has been obtained as [20]

$$\begin{aligned} G &= H - TS = M - TS \\ &= \frac{3Q^2}{4r_+} + \frac{r_+}{4} - \frac{2P\pi r_+^3}{3} - \frac{a(2+3\omega_q)}{4r_+^{3\omega_q}}. \end{aligned} \tag{9}$$

Note that the mass has been interpreted as enthalpy in the extended phase space [1].

P-V criticality is discussed in detail in Ref. [20]. It is worth mentioning that we can obtain the analytic expression of critical quantities when $\omega_q = -2/3$ as follows:

$$v_c = 2\sqrt{6}Q, \quad T_c = \frac{\sqrt{6}}{18\pi Q} - \frac{a}{2\pi}, \quad P_c = \frac{1}{96\pi Q^2}, \tag{10}$$

where v_c, T_c, and P_c denote the critical specific volume, critical Hawking temperature, and critical thermodynamic pressure, respectively. When $\omega_q \neq -2/3$, critical quantities can be obtained numerically for different choices of parameters.

III. DYNAMIC PHASE TRANSITION OF THE RN-ADS BLACK HOLE SURROUNDED BY QUINTESSENCE

A. Gibbs free energy landscape for the RN-AdS black hole surrounded by quintessence

In the P-V criticality research [4], Gibbs free energy plays a very important role by identifying the first-order phase transition via the classical swallowtail behavior. In the pioneering works of black hole dynamic phase transition [14,15], Gibbs free energy also plays a crucial role. The analysis of dynamic phase transition is based on the so-called "Gibbs free energy landscape", where Gibbs free

energy G_L has a similar definition as Eq. (9) other than the replacement of the Hawking temperature T with the temperature of the ensemble T_E. Here, we consider the canonical ensemble at the specific temperature T_E composed by a series of black holes with an arbitrary horizon radius. It was argued that G_L describes a real black hole only when $T_E = T$ [14,15]. It was further proved that only the extremal points of G_L make sense with the local minimum and maximum corresponding to the stable and unstable phases respectively.

Utilizing Eqs. (4), (6), and (7), we can obtain the expression of Gibbs free energy G_L on the Gibbs free energy landscape as

$$G_L = H - T_E S = \frac{r_+}{2}\left(1 + \frac{Q^2}{r_+^2} - \frac{a}{r_+^{3\omega_q+1}} + \frac{8\pi P r_+^2}{3} - 2\pi r_+ T_E\right). \quad (11)$$

To gain an intuitive understanding, we present a specific example in Fig. 1. From the G-T graph on the left side, it can be witnessed that there exists three branches; namely, the large black hole branch, the intermediate black hole branch, and the small black hole branch. The swallow tail behavior which is characteristic of first-order phase transition appears when the pressure is fixed at a value lower than the critical thermodynamic pressure. We can read off the phase transition temperature from the intersection point between the large black hole branch and the small black hole branch as 0.0285. Note that in the following investigation of dynamic phase transition, we will consider the case $T_E = 0.0285$ for consistency. From the right graph, one can see clearly there exist double wells in the $G_L - r_+$ curve. Note that these two wells have the same depth.

B. Probabilistic evolution of the RN-AdS black hole surrounded by quintessence

Considering the thermal fluctuation, we can define in the canonical ensemble a probability distribution of black hole states with respect to the horizon radius. Namely, $\rho(r_+)$. Given the initial distribution, we can probe its evolution with time in the Gibbs free energy landscape. Then it should be a function of both the black hole horizon radius r_+ and time t can be expressed as $\rho(r_+, t)$.

As a useful tool to probe the probabilistic evolution of the black hole, Fokker-Planck equation reads [43–47]

$$\frac{\partial \rho(r_+,t)}{\partial t} = D\frac{\partial}{\partial r_+}\left\{e^{-\beta G_L(T,P,r_+)}\frac{\partial}{\partial r_+}[e^{\beta G_L(T,P,r_+)}\rho(r_+,t)]\right\}. \quad (12)$$

The parameter $\beta = \frac{1}{k_B T}$ and the diffusion coefficient $D = \frac{k_B T}{\zeta}$, where ζ and k_B are the dissipation coefficient and Boltzman constant, respectively. Both k_B and ζ can be set to one without loss of generality.

We can obtain the time evolution picture of the probability distribution by numerically solving Eq. (12). Note that there are several types of boundary conditions; reflecting boundary condition, absorbing boundary condition, periodic boundary condition, etc. The boundary conditions are chosen correspondingly considering the nature of the problem. Since G_L here does not possess the periodic property, we would not consider the periodic boundary condition. Here, we consider the reflecting boundary condition because it can ensure the normalization of ρ. As proposed in Ref. [15], the reflecting boundary condition can be imposed as $\beta G'(r_+)\rho(r_+,t) + \rho'(r_+,t)|_{r_+=r_0} = 0$. It can be derived by letting the expression inside the brace of the right-hand side of Eq. (12) equal zero. Since the Gibbs free energy is divergent at $r_+ = 0$ and $r_+ = +\infty$, the reflecting boundary condition should be carefully considered to avoid numerical instability. As shown in Fig. 2, we plot the evolution of $\rho(r_+, t)$ for the RN-AdS black hole surrounded by quintessence with $Q = 1$, $T_E = 0.0285$. In the top rows, the parameters of a and ω_q are chosen as 0 and 0, respectively. In the bottom

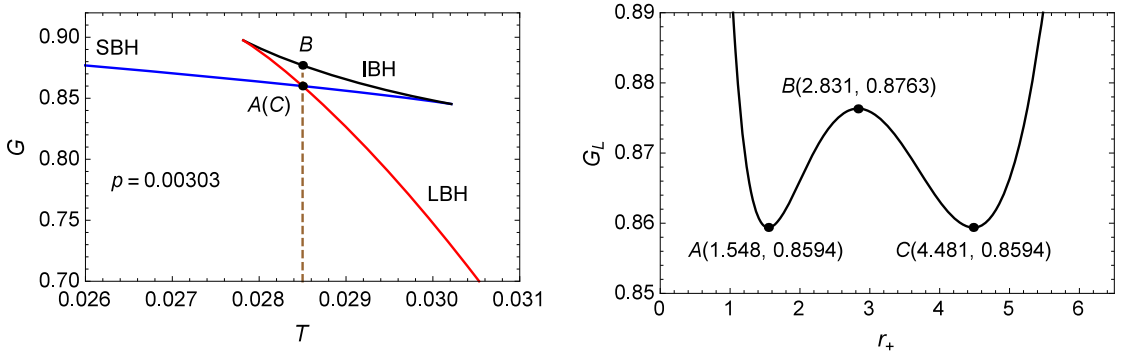

(a) (b)

FIG. 1. Gibbs free energy for the RN-AdS black hole surrounded by quintessence with $Q = 1$, $\omega_q = -0.78$, $a = 0.05$, $P = 0.00303$. (a) $G - T$ graph (b) G_L vs r_+ when $T_E = 0.0285$.

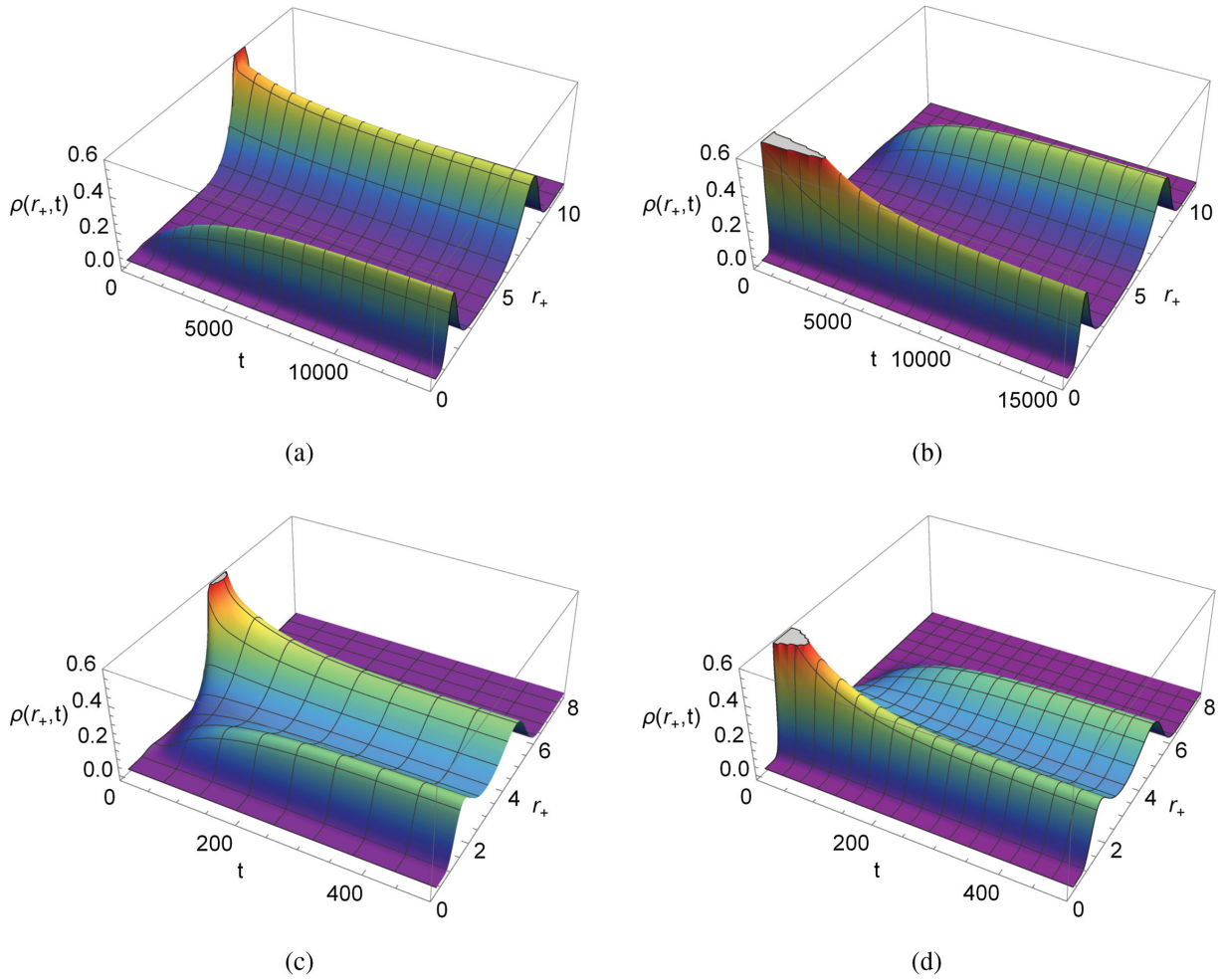

FIG. 2. Time evolution of $\rho(r_+, t)$ for the RN-AdS black hole surrounded by quintessence with $Q = 1$, $T_E = 0.0285$. (a) $a = 0$ (b) $a = 0$ (c) $a = 0.05$, $\omega_q = -0.78$ (d) $a = 0.05$, $\omega_q = -0.78$. For the left two graphs, the initial condition is chosen as a Gaussian wave pocket located at the large black hole state while for the right two graphs, the initial condition is chosen as a Gaussian wave pocket located at the small black hole state.

rows, the parameters of a and ω_q are chosen as 0.05 and -0.78, respectively. For the left two graphs, the initial condition is chosen as a Gaussian wave pocket located at the large black hole state $\{\rho(r_+, 0) = \frac{1}{\sqrt{\pi}b} e^{-(r_+ - r_{+l})^2/b^2}$ [15], where r_{+l} denotes the horizon radius of large black hole$\}$ while for the right two graphs, the initial condition is chosen as a Gaussian wave pocket located at the small black hole state $\{\rho(r_+, 0) = \frac{1}{\sqrt{\pi}b} e^{-(r_+ - r_{+s})^2/b^2}$ [15], where r_{+s} denotes the horizon radius of small black hole$\}$. Here, we use the notation b instead of a in Ref. [15] to avoid confusion with the normalization factor a which is related to the density of quintessence.

Figure 2 allows one to gain an overall picture of how the probability distribution $\rho(r_+, t)$ evolves. For a precise understanding, we plot the time evolution of both $\rho(r_{+l}, t)$ and $\rho(r_{+s}, t)$ in Fig. 3. The parameters here are chosen the same as Fig. 2. Also, the initial condition is chosen as a Gaussian wave pocket located at the large black hole state for the left two graphs while the initial condition is chosen as Gaussian wave pocket located at the small black hole state for the right two graphs.

As can be seen from Figs. 2(a) and 2(c) where the initial state is the large black hole, the peak denoting the large black hole gradually decreases while the other peak denoting the small black hole starts to grow from zero. Also, $\rho(r_+, t)$ approaches a stationary distribution in the long time limit with two peaks denoting the large and small black holes, respectively. This clearly exhibits the dynamic process of how the initial large black hole evolves into the small black hole. Similar analysis is applicable when the initial black hole state is a small black hole. It is worth pointing out that although the final probability distribution does not rely on the initial condition and the location of two peaks would not change with the initial condition, the values of the two peaks would change slightly. This is because $\rho(r_+, t)$ is not strictly normalized in the numerics treatment.

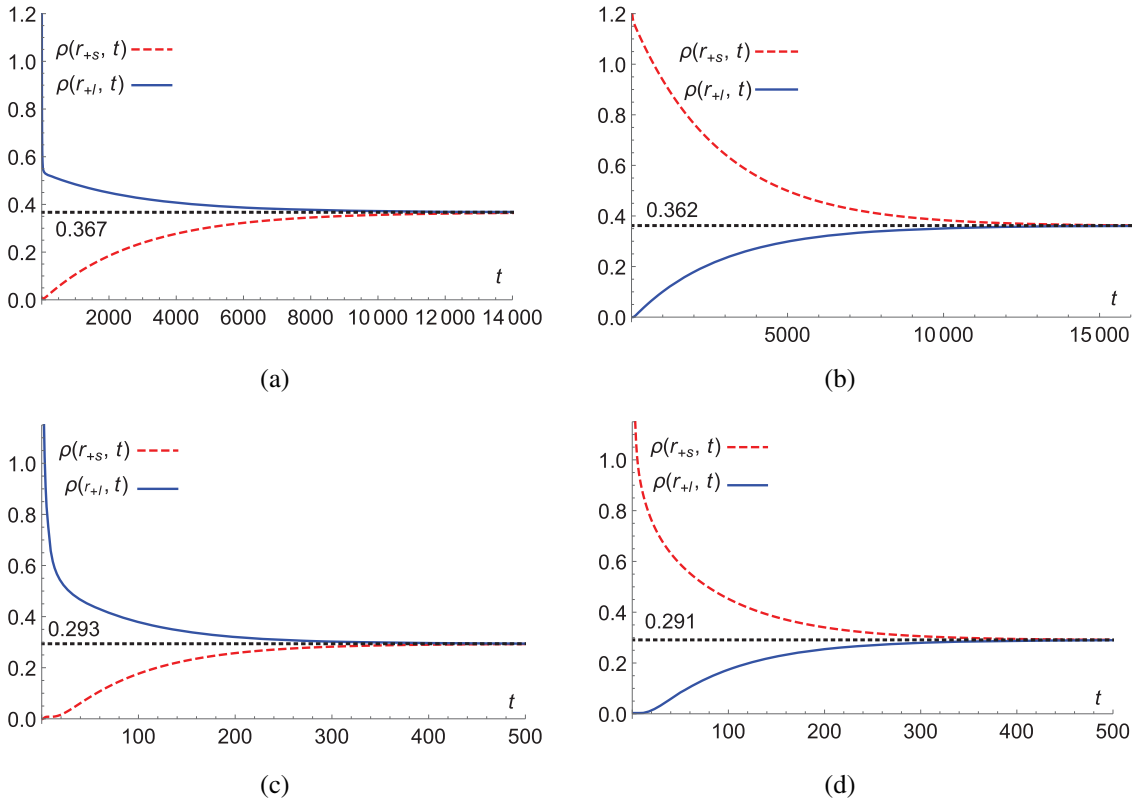

FIG. 3. Time evolution of $\rho(r_{+l}, t)$ and $\rho(r_{+s}, t)$ for the RN-AdS black hole surrounded by quintessence with $Q = 1$, $T_E = 0.0285$. (a) $a = 0$ (b) $a = 0$ (c) $a = 0.05$, $\omega_q = -0.78$ (d) $a = 0.05$, $\omega_q = -0.78$. For the left two graphs, the initial condition is chosen as a Gaussian wave pocket located at the large black hole state while for the right two graphs, the initial condition is chosen as a Gaussian wave pocket located at the small black hole state.

More specifically, the evolution of both the $\rho(r_{+l}, t)$ and $\rho(r_{+s}, t)$ can be reflected in Figs. 3(a) and 3(c). At first, $\rho(r_{+l}, t)$ is finite while $\rho(r_{+s}, t)$ equals to zero. During the evolution, $\rho(r_{+l}, t)$ decreases while $\rho(r_{+s}, t)$ increases. Finally, they approach to the same value (0.367 for the case of $a = 0$ and 0.293 for the case of $\omega_q = -0.78$), consistent with the conclusion in Ref [17] that the final probability of the large black hole equals to that of the small black hole because their Gibbs free energy are equal to each other.

Comparing the top two graphs with the bottom two graphs in both Figs. 2 and 3, we can see that the initial black hole state evolves more quickly in the case with dark energy than in the case without dark energy. So this phenomenon reflects the effect of quintessence dark energy on the dynamic phase transition of black holes.

C. First passage process for the phase transition of the RN-AdS black hole surrounded by quintessence

The first passage process for a black hole phase transition describes a process where the initial small (large) black hole state reaches the intermediate transition state for the first time. This process can be interpreted intuitively from the Gibbs free energy landscape where for the first time the state at the well of G_L reaches the state at the barriers of G_L. The corresponding time for this process is called the first passage time.

In order to probe the dynamic evolution of $\rho(r_+, t)$ in the first passage process, we need to resolve the Fokker-Planck equation by adding the absorbing boundary condition $\{\rho(r_{+m}, t) = 0$ [15]$\}$ for the intermediate transition state (the Gibbs free energy achieves the local maximum here) in addition to the reflecting boundary condition mentioned in the former subsection. r_{+m} denotes the horizon radius corresponding to the intermediate transition state. Recall that we have solved the Fokker-Planck equation with only the reflecting boundary conditions in the former subsection. We plot the evolution of $\rho(r_+, t)$ in the first passage process for the RN-AdS black hole surrounded by quintessence with $Q = 1$, $T_E = 0.0285$ in Fig. 4. For the left two graphs, the initial condition is chosen as a Gaussian wave pocket located at the large black hole state while for the right two graphs; the initial condition is chosen as the Gaussian wave pocket located at the small black hole state. In the top rows, the parameters of a and ω_q are chosen as 0 and 0, respectively. In the bottom rows, the parameters of a and ω_q are chosen as 0.05 and -0.78, respectively. As shown in Fig. 4, the peaks located at the large (small) black

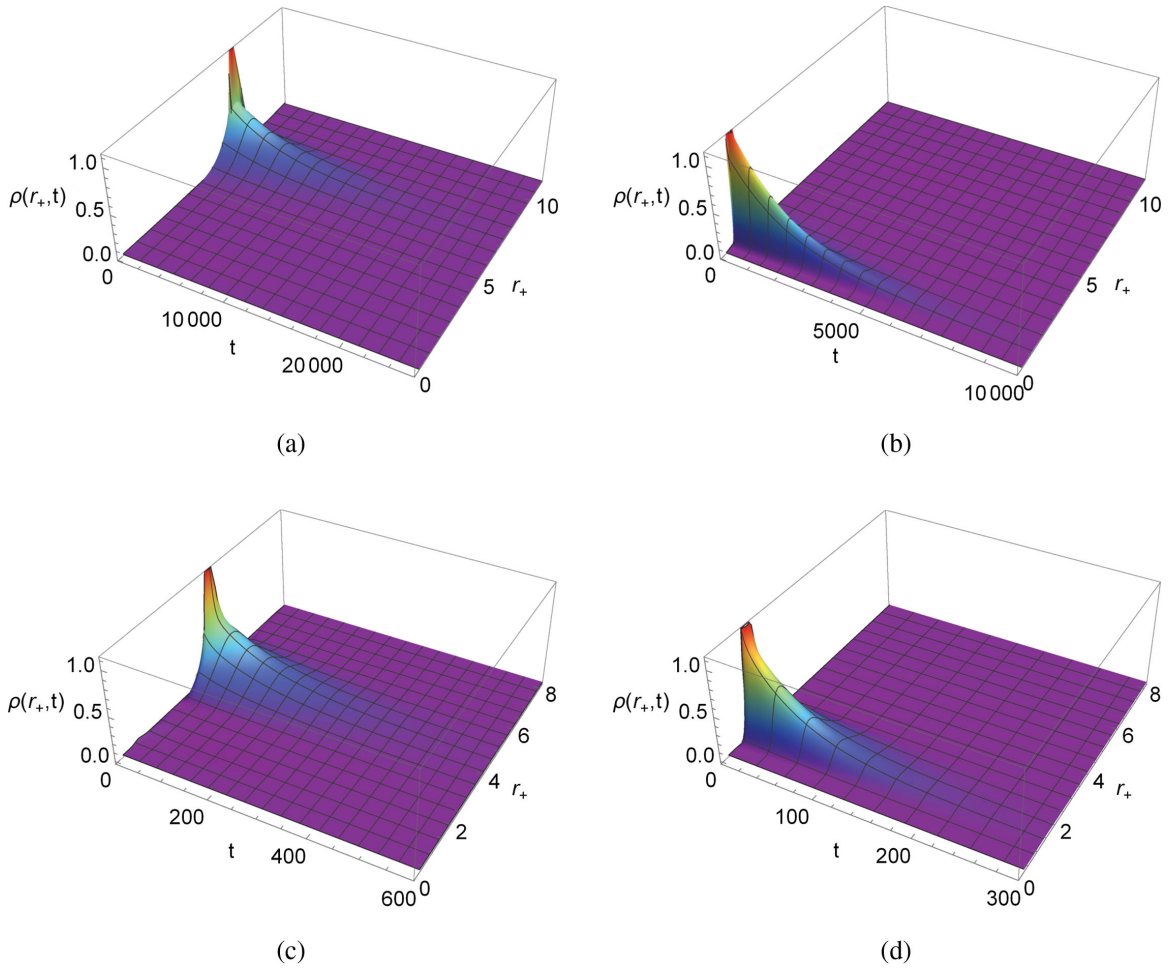

FIG. 4. Time evolution of $\rho(r_+, t)$ in the first passage process of the RN-AdS black hole surrounded by quintessence with $Q = 1$, $T_E = 0.0285$. (a) $a = 0$ (b) $a = 0$ (c) $a = 0.05$, $\omega_q = -0.78$ (d) $a = 0.05$, $\omega_q = -0.78$. For the left two graphs, the initial condition is chosen as the Gaussian wave pocket located at the large black hole state while for the right two graphs, the initial condition is chosen as the Gaussian wave pocket located at the small black hole state.

hole decay very rapidly, irrespective of the initial black hole state. The peaks of the case with dark energy decays more rapidly than that of the case without dark energy, showing the effect of quintessence dark energy.

Consider the probability that by time t the black hole system still stays at the large or small black hole state (not having accomplished a first passage) and can be added up as $\Sigma(t)$, then the distribution of first passage time [denoted as $F_p(t)$] reads [14]

$$F_p(t) = -\frac{d\Sigma(t)}{dt}. \tag{13}$$

The behavior of $\Sigma(t)$ is depicted in Fig. 5. Regardless what the initial black hole state is, $\Sigma(t)$ decreases quickly, implying that the transition from the large (small) black hole state to the small (large) black hole state happens quickly.

Utilizing the Fokker-Planck equation and Eq. (13), the relation between $F_p(t)$ and $\rho(r_+, t)$ has been derived as [15]

$$F_p(t) = -D\frac{\partial\rho(r_+, t)}{\partial r_+}\bigg|_{r_m}, \tag{14}$$

We plot $F_p(t)$ in Fig. 6. A single peak can be found in all four cases, implying that considerable first passage events happen at short time. From Figs. 5 and 6, we can see clearly that the initial black hole state evolves more quickly in the case with dark energy than in the case without dark energy, consistent with the observations of Figs. 2–4.

With the time distributions, we can calculate the mean first passage time, whose definition is as follows:

$$\langle t\rangle = \int_0^\infty tF_p(t)dt. \tag{15}$$

To further probe the effect of quintessence dark energy on the dynamic phase transition of black holes, we investigate the relation between the mean first passage time and the height of the barrier for various choices of

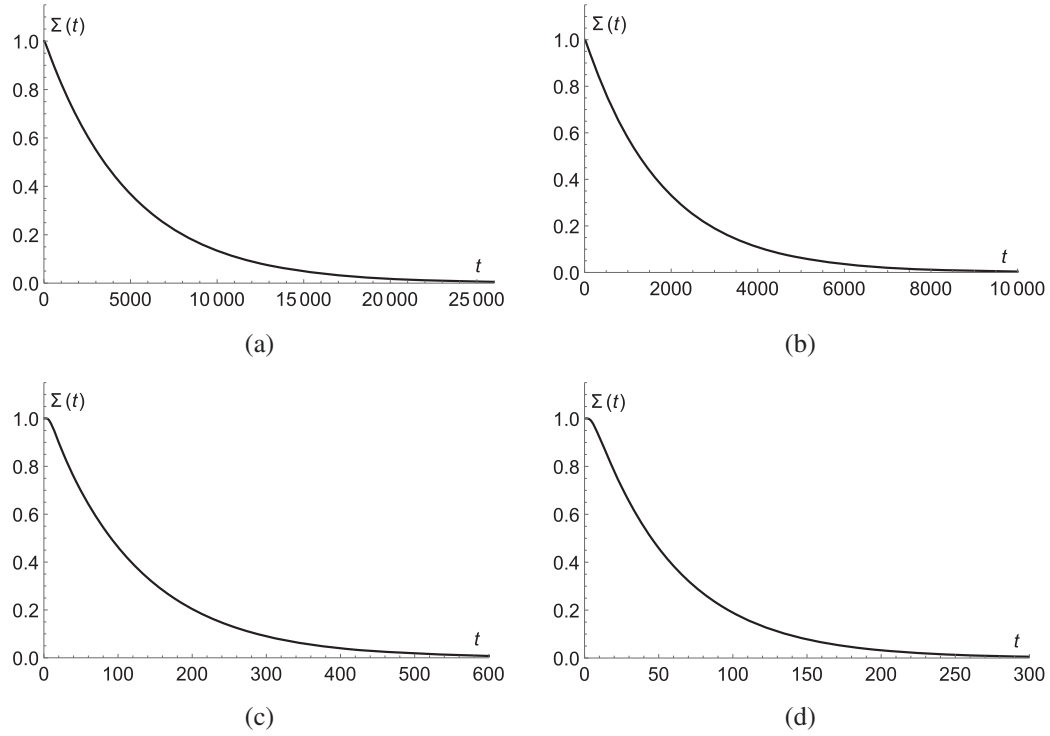

FIG. 5. Time evolution of $\Sigma(t)$ for the RN-AdS black hole surrounded by quintessence with $Q = 1$, $T_E = 0.0285$. (a) $a = 0$ (b) $a = 0$ (c) $a = 0.05$, $\omega_q = -0.78$ (d) $a = 0.05$, $\omega_q = -0.78$. For the left two graphs, the initial condition is chosen as a Gaussian wave pocket located at the large black hole state while for the right two graphs, the initial condition is chosen as a Gaussian wave pocket located at the small black hole state.

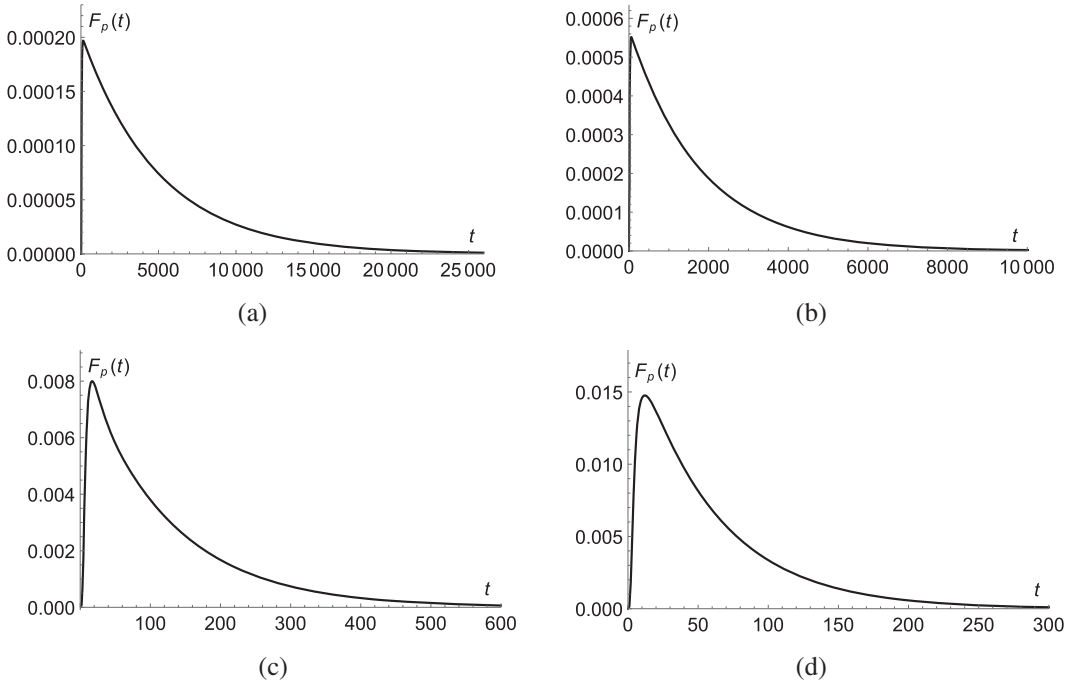

FIG. 6. $F_p(t)$ for the RN-AdS black hole surrounded by quintessence with $Q = 1$, $T_E = 0.0285$. (a) $a = 0$ (b) $a = 0$ (c) $a = 0.05$, $\omega_q = -0.78$ (d) $a = 0.05$, $\omega_q = -0.78$. For the left two graphs, the initial condition is chosen as a Gaussian wave pocket located at the large black hole state while for the right two graphs, the initial condition is chosen as a Gaussian wave pocket located at the small black hole state.

TABLE I. The mean first passage time and the height of the barrier ΔG_L.

ω_q	/	−0.34	−0.4	−0.5	−0.6	−0.7	−0.75	−0.78	−0.8	−0.9	−0.95	−0.99
a	0	0.05	0.05	0.05	0.05	0.05	0.05	0.05	0.05	0.05	0.05	0.05
$G_L(B)$	1.0137	0.9391	0.9260	0.9037	0.8853	0.8758	0.8755	0.8770	0.8788	0.9025	0.9334	0.9886
$G_L(A/C)$	0.8943	0.8613	0.8597	0.8572	0.8556	0.8564	0.8583	0.8600	0.8615	0.8729	0.8819	0.8914
$\Delta G_L = G_L(B) - G_L(A/C)$	0.1194	0.0778	0.0663	0.0465	0.0297	0.0194	0.0172	0.0170	0.0173	0.0296	0.0515	0.0972
$\langle t \rangle\|_{\mathrm{LBH}\to\mathrm{SBH}}$	4839	1322	919	466	242	147	127	122	124	197	439	2124
$\langle t \rangle\|_{\mathrm{SBH}\to\mathrm{LBH}}$	1846	523	371	198	110	72	65	61	63	96	196	957

parameter ω_q. As can be seen from Table I, the mean first passage time for the case with dark energy is much shorter than that of the case without dark energy, showing the influence of quintessence dark energy. This can be attributed to the finding that the height of the barrier for the case with dark energy is lower than that of the case without dark energy. Interestingly enough, the effect of dark energy is quite unique. For the range of ω_q, there exists a minimum mean first passage time. With the increasing of the ω_q from −0.99 to −0.34, the mean first passage time decreases dramatically and then increases. Considering the mean first passage time is an observable of black hole dynamic phase transition; the unique results we obtain here may shed new light on constraining the parameters of the quintessence dark energy theory based on the observation.

IV. CONCLUSIONS

We investigate in detail the dynamic phase transition of charged AdS black holes surrounded by quintessence in this paper and disclose the effect of quintessence dark energy on the kinetics of the phase transition.

First, we obtain the analytic expression of Gibbs free energy G_L for charged AdS black holes surrounded by quintessence based on the Gibbs free energy landscape. We read off the phase transition temperature from the intersection point between the large black hole branch and the small black hole branch. Then we plot the $G_L - r_+$ curve at the phase transition temperature. As clearly shown in the $G_L - r_+$ curve, there exist double wells which have the same depth.

Second, by numerically solving the Fokker-Planck equation with both the initial condition and reflecting boundary condition imposed, we probe the probabilistic evolution of charged AdS black holes surrounded by quintessence. We display the evolution of the probability distribution $\rho(r_+, t)$ graphically. We also plot the time evolution of both $\rho(r_{+l}, t)$ and $\rho(r_{+s}, t)$. These two sets of figures are mutually complementary with each other. For the case where the initial state is the large black hole, the peak denoting the large black hole gradually decreases while the other peak denoting the small black hole starts to grow from zero. Additionally, $\rho(r_+, t)$ approaches becoming a stationary distribution in the long time limit with two peaks denoting the large and small black holes respectively. This clearly demonstrates the dynamic process of how the initial large black hole evolves into the small black hole. More specifically, $\rho(r_{+l}, t)$ is finite while $\rho(r_{+s}, t)$ equals zero at the begining. During the evolution, $\rho(r_{+l}, t)$ decreases while $\rho(r_{+s}, t)$ increases. Finally, they approach to the same value. Similar explanations are applicable when the initial black hole state is a small black hole. We stress that the effect of quintessence dark energy on the dynamic phase transition of black holes can be clearly reflected in the above process. The initial black hole state evolves more quickly in the case with dark energy than in the case without dark energy.

Third, we consider the first passage process which describes the process that the small (large) black hole state reaches the intermediate transition state for the first time. The corresponding time is called the first passage time. We resolve the Fokker-Planck equation by adding the absorbing boundary condition for the intermediate transition state. It is shown intuitively that the peaks located at the large (small) black hole decay very rapidly, irrespective of the initial black hole state. The corresponding peak in the case with dark energy decays more quickly than that in the case without dark energy. Moreover, we discuss the quantity $\Sigma(t)$ which add up the probability that by time t the black hole system still stays at the large or small black hole state (not having accomplished a first passage). It is shown that $\Sigma(t)$ decreases quickly no matter what the initial black hole state is, suggesting that the transition from the large (small) black hole state to the small (large) black hole state happens quickly. It can also be witnessed from the distribution of the first passage time $F_p(t)$.

Last but not least, we investigate the relation between the mean first passage time and the height of the barrier for various choices of parameter ω_q. It is shown that the mean first passage time for the case with dark energy is much shorter than that of the case without dark energy, which can be interpreted by the finding that the height of the barrier for the case with dark energy is lower than that of the case without dark energy. Interestingly enough, the effect of dark energy is quite unique. For the range of ω_q, there exists a minimum mean first passage time. With the increasing of the ω_q from −0.99 to −0.34, the mean first

passage time decreases dramatically and then increases. Considering the mean first passage time is an observable of black hole dynamic phase transition, the unique results we obtain here may shed new light on the constraining the parameters of the quintessence dark energy theory based on the future observation.

For further investigation, one can consider the case that the initial Gaussian wave packet is not chosen at large/small black hole state. One can also probe the dynamic evolution from the unstable black hole to the stable black hole.

ACKNOWLEDGMENTS

Shan-Quan Lan is supported by National Natural Science Foundation of China (Grant No. 12005088) and the Lingnan Normal University Project (Grants No. YL20200203 and No. ZL1930). G.-Q. L. is supported by Guangdong Basic and Applied Basic Research Foundation, China (Grant No. 2021A1515010246). The authors would like to express their sincere gratitude to the anonymous referees whose insightful suggestions have help improved the quality of this paper significantly.

[1] D. Kastor, S. Ray, and J. Traschen, Enthalpy and the mechanics of AdS black holes, Classical Quantum Gravity **26**, 195011 (2009).
[2] B. Dolan, The cosmological constant and the black hole equation of state, Classical Quantum Gravity **28**, 125020 (2011).
[3] B. P. Dolan, Pressure and volume in the first law of black hole thermodynamics, Classical Quantum Gravity **28**, 235017 (2011).
[4] D. Kubizňák and R. B. Mann, *P-V* criticality of charged AdS black holes, J. High Energy Phys. 07 (2012) 033.
[5] A. Chamblin, R. Emparan, C. V. Johnson, and R. C. Myers, Charged AdS black holes and catastrophic holography, Phys. Rev. D **60**, 064018 (1999).
[6] A. Chamblin, R. Emparan, C. V. Johnson, and R. C. Myers, Holography,thermodynamics and fluctuations of charged AdS black holes, Phys. Rev. D **60**, 104026 (1999).
[7] N. Altamirano, D. Kubizňák, R. Mann, and Z. Sherkatghanad, Reentrant phase transitions in rotating antiCde Sitter black holes, Phys. Rev. D **88**, 101502 (2013).
[8] N. Altamirano, D. Kubizňák, R. Mann, and Z. Sherkatghanad, Kerr-AdS analogue of tricritical point and solid/liquid/gas phase transition, Classical Quantum Gravity **31**, 042001 (2014).
[9] S. W. Wei and Y. X. Liu, Triple points and phase diagrams in the extended phase space of charged Gauss-Bonnet black holes in AdS space, Phys. Rev. D **90**, 044057 (2014).
[10] R. A. Hennigar, R. B. Mann, and E. Tjoa, Superfluid black holes, Phys. Rev. Lett. **118**, 021301 (2017).
[11] A. Dehghani, S. H. Hendi, and R. B. Mann, Range of novel black hole phase transitions via massive gravity: Triple points and *N*-fold reentrant phase transitions, Phys. Rev. D **101**, 084026 (2020).
[12] N. Altamirano, D. Kubizňák, R. Mann, and Z. Sherkatghanad, Thermodynamics of rotating black holes and black rings: Phase transitions and thermodynamic volume, Galaxies **2**, 89 (2014).
[13] D. Kubizňák, R. Mann, and M. Teo, Black hole chemistry: Thermodynamics with Lambda, Classical Quantum Gravity **34**, 063001 (2017).
[14] R. Li and J. Wang, Thermodynamics and kinetics of Hawking-Page phase transition, Phys. Rev. D **102**, 024085 (2020).
[15] R. Li, K. Zhang, and J. Wang, Thermal dynamic phase transition of Reissner-Nordström Anti-de Sitter black holes on free energy landscape, J. High Energy Phys. 10 (2020) 090.
[16] R. Li and J. Wang, Energy and entropy compensation, phase transition and kinetics of four dimensional charged Gauss-Bonnet Anti-de Sitter black holes on the underlying free energy landscape, arXiv:2012.05424.
[17] S. W. Wei, Y. Q. Wang, Y. X. Liu, and R. B. Mann, Dynamic properties of thermodynamic phase transition for five-dimensional neutral Gauss-Bonnet AdS black hole on free energy landscape, arXiv:2009.05215.
[18] S. W. Wei, Y. Q. Wang, Y. X. Liu, and R. B. Mann, Observing dynamic oscillatory behavior of triple points among black hole thermodynamic phase transitions, Sci. China Phys. Mech. Astron. **64**, 270411 (2021).
[19] R. Li, K. Zhang, and J. Wang, Probing black hole microstructure with the kinetic turnover of phase transition, arXiv:2102.09439 [Phys. Rev. D (to be published)].
[20] G. Q. Li, Effects of dark energy on *PCV* criticality of charged AdS black holes, Phys. Lett. B **735**, 256 (2014).
[21] S. Tsujikawa, Quintessence: A review, Classical Quantum Gravity **30**, 214003 (2013).
[22] Y. Fujii, Origin of the gravitational constant and particle masses in a scale-invariant scalar-tensor theory, Phys. Rev. D **26**, 2580 (1982).
[23] L. H. Ford, Cosmological-constant damping by unstable scalar fields, Phys. Rev. D **35**, 2339 (1987).
[24] C. Wetterich, Cosmology and the fate of dilatation symmetry, Nucl. Phys. **B302**, 668 (1988).
[25] B. Ratra and P. J. E. Peebles, Cosmological consequences of a rolling homogeneous scalar field, Phys. Rev. D **37**, 3406 (1988).
[26] V. V. Kiselev, Quintessence and black holes, Classical Quantum Gravity **20**, 1187 (2003).
[27] S. B. Chen and J. L. Jing, Quasinormal modes of a black hole surrounded by quintessence, Classical Quantum Gravity **22**, 4651 (2005).

[28] S. Chen, B. Wang, and R. Su, Hawking radiation in a d-dimensional static spherically-symmetric black Hole surrounded by quintessence, Phys. Rev. D **77**, 124011 (2008).
[29] G. Q. Li and S. F. Xiao, State equations for massless spin fields in static spherical spacetime filled with quintessence, Gen. Relativ. Gravit. **42**, 1719 (2010).
[30] S. Fernando, Schwarzschild black hole surrounded by quintessence: Null geodesics, Gen. Relativ. Gravit. **44**, 1857 (2012).
[31] M. A. Aïnou and M. E. Rodrigues, Thermodynamical, geometrical and Poincar methods for charged black holes in presence of quintessence, J. High Energy Phys. 09 (2013) 146.
[32] C. Ding, C. Liu, Y. Xiao, L. Jiang, and R. G. Cai, Strong gravitational lensing in a black-hole spacetime dominated by dark energy, Phys. Rev. D **88**, 104007 (2013).
[33] M. Azreg-Aïnou, Black hole thermodynamics: No inconsistency via the inclusion of the missing $P - V$ terms, Phys. Rev. D **91**, 064049 (2015).
[34] X. X. Zeng, D. Y. Chen, and L. F. Li, Holographic thermalization and gravitational collapse in a spacetime dominated by quintessence dark energy, Phys. Rev. D **91**, 046005 (2015).
[35] M. Cvetic, G. W. Gibbons, and C. N. Pope, Photon spheres and sonic horizons in black holes from supergravity and other theories, Phys. Rev. D **94**, 106005 (2016).
[36] X. X. Zeng and L. F. Li, Van der Waals phase transition in the framework of holography, Phys. Lett. B **764**, 100 (2017).
[37] Z. Xu and J. Wang, Kerr-Newman-AdS black hole in quintessential dark energy, Phys. Rev. D **95**, 064015 (2017).
[38] H. Liu and X. H. Meng, Effects of dark energy on the efficiency of charged AdS black holes as heat engines, Eur. Phys. J. C **77**, 556 (2017).
[39] J. de Oliveira and R. D. B. Fontana, Three-dimensional black holes with quintessence, Phys. Rev. D **98**, 044005 (2018).
[40] K. J. He, X. Y. Hu, and X. X. Zeng, Weak cosmic censorship conjecture and thermodynamics in quintessence AdS black hole under charged particle absorption, Chin. Phys. C **43**, 125101 (2019).
[41] X. Y. Guo, H. F. Li, L. C. Zhang, and R. Zhao, Continuous phase transition and microstructure of charged AdS black hole with quintessence, Eur. Phys. J. C **80**, 168 (2020).
[42] D. W. Yan, Z. R. Huang, and N. Li, Phase transition, Hawking-Page phase transitions of charged AdS black holes surrounded by quintessence, Chin. Phys. C **45**, 015104 (2021).
[43] R. Zwanzig, *Nonequilibrium Statistical Mechanics* (Oxford University Press, New York, 2001).
[44] C.-L. Lee, C.-T. Lin, G. Stell, and J. Wang, Diffusion dynamics, moments, and distribution of first-passage time on the protein-folding energy landscape, with applications to single molecules, Phys. Rev. E **67**, 041905 (2003).
[45] C.-L. Lee, G. Stell, and J. Wang, First-passage time distribution and non-Markovian diffusion dynamics of protein folding, J. Chem. Phys. **118**, 959 (2003).
[46] J. Wang, Landscape and flux theory of non-equilibrium dynamical systems with application to biology, Adv. Phys. **64**, 1 (2015).
[47] J. D. Bryngelson and P. G. Wolynes, Intermediates and barrier crossing in a random energy model (with applications to protein folding), J. Phys. Chem. **93**, 6902 (1989).